Catalysis Letters, Vol. 118, Nos. 1–2, October 2007 (© 2007)
DOI: 10.1007/s10562-007-9139-0

Synthesis and catalytic performance of gold-loaded TiO_2 nanofibers

Baolin Zhu, Kairong Li, Yunfeng Feng, Shoumin Zhang, Shihua Wu, and Weiping Huang*

Department of Chemistry, Nankai University, Tianjin, 300071, China

Received 15 April 2007; accepted 7 May 2007

By using titanate nanotubes and $HAuCl_4$ as precursor, gold-loaded TiO_2 nanofibers (Au/TiO_2NFs) are obtained after deposition-photodecomposition process, and the tubular supports are broken after the fabrication process. Catalytic performance of the obtained Au/TiO_2NFs is evaluated for low-temperature CO oxidation and photodegradation of methyl orange under UV illumination, and the relationship between the catalytic activity and calcination treatment is investigated. After the Au/TiO_2NFs are calcined, their catalytic activity for CO oxidation is enhanced, while the photocatalytic activity decreases.

KEY WORDS: gold; TiO_2 nanofibers; catalytic activity; CO oxidation; photodegradation.

1. Introduction

Gold has been generally regarded as an inert metal until its surprisingly high activity for low-temperature CO oxidation is reported by Haruta and co-workers [1]. Following this work, highly-dispersed gold nanoparticles has been explored to be active in several reactions, including CO oxidation, propylene epoxidation, methanol synthesis, water gas shift reaction, preferential oxidation of CO in the presence of excess hydrogen, environmental catalysis (NO_x reduction), hydrogenation reactions, etc. [2]. For supported gold catalysts, different supports have been intensively researched, and their cooperative effects with gold particles are also investigated [3–5]. Among them, TiO_2 is a prominent one owing to its low-cost, innocuity, and stability [6]. Recent investigations on gold–TiO_2 nanocomposite also show that gold-doping enhances the photocatalytic activity and extends the response of the TiO_2 catalyst into visible region [7]. It has been well established that the catalytic properties of Au–TiO_2 system depends not only on the size of the Au clusters, the preparation method, but also the support [8]. TiO_2 nanotube, which has large surface area, should be a better support than common TiO_2 powder. In 1998, Kasuga developed a hydrothermal method to turn TiO_2 powders into tubular structure in 10 M NaOH solution [9]. In our earlier work, gold particles are loaded on this kind of nanotubes by deposition-precipitation method [10], and CuO-modified ones are prepared by impregnation method [11]. All of the prepared catalysts exhibit high catalytic activity for low-temperature CO oxidation after a calcinations process [10,11], which indicates the application potential of TiO_2 nanotubes in the catalyst field. In this letter, gold particles are loaded on titanate nanotubes by deposition-photodecomposition method. Their catalytic activity for CO oxidation and photodegradation of methyl orange is evaluated.

*To whom correspondence should be addressed.
E-mail: huangw@eyou.com

2. Experimental

2.1. Preparation of samples

Pure anatase TiO_2 powder is dispersed in an aqueous solution of NaOH (10 M) and charged into a Teflon-lined autoclave. The autoclave is heated in an oil bath at 150 °C for 12 h. Prepared sample is washed with 0.1 M HCl solution and water, respectively. White titanate nanotubes (denoted as Sample **a**) are obtained after they are dried at 80 °C in air. The nanotubes are first dispersed in water (1 g TiO_2 nanotubes/100 mL H_2O) and then appropriate $HAuCl_4$ solution (0.21 mg/mL) is added. The solution is adjusted to pH = 7 with $NH_3 \cdot H_2O$. Then the suspension is irradiated for 6 h by using a 300 W High-pressure Mercury Lamp at a distance of 10 cm under stirring at ambient temperature. Obtained purple Au/TiO_2NFs (denoted as Sample **b**) are washed with water to remove Cl^- ions and dried at 80 °C in air. Sample **c** is obtained after Sample **b** is calcined at 300 °C for 3 h. The calculated gold content is 1 wt.%.

2.2. Sample characterization

The powder X-ray diffraction (XRD) experiments are carried out at room temperature using a Rigaku D/Max-2500 X-ray diffractometer (CuKα λ = 0.154 nm) to identify crystal phase of the products. Diffraction peaks of crystalline phases are compared with those reported in the JCPDS Data File. TEM images are

obtained with a Philips T20ST transmission electron microscopy working at 200 kV.

2.3. Catalytic activity

Catalytic performance of the samples for low-temperature CO oxidation is tested using a fixed bed flow microreactor (7 mm i.d.) under atmospheric pressure using 100 mg catalyst powder. Reaction gas mixture consisting of 1% CO balanced with air is passed through the catalyst bed at a total flow rate of 33.6 mL/min. The composition of reactant and product is analyzed on-line with a GC-508A gas chromatograph equipped with a thermal conductivity detector (TCD) $T_{50\%}$ is the temperature for 50% CO conversion on catalyst.

Photocatalytic activity experiments for the degradation of methyl orange in water are performed in a UV-light reactor. 50 mg photocatalyst is dispersed in 100 mL methyl orange solution (13 mg/L). The reactor is illuminated with a 300 W high-pressure mercury lamp at a distance of 10 cm under ambient condition. The concentration of methyl orange solution is monitored by measuring the absorption at 463.5 nm using a TU-1901 spectrometer. The results are corrected for the decomposition of the dye in the absence of catalysts and adsorption of dye on the catalyst.

3. Results and discussion

3.1. Microstructural characterization of the samples

To determine the crystal structure of the products, powder XRD is carried out. The patterns of all the samples are shown in figure 1. It can be observed that crystal phase of the nanotube support changes obviously after the deposition-photodecomposition process. From curve **a**, it can be found that TiO_2 nanotubes are composed of titanate $H_2Ti_2O_5 \cdot H_2O$ (JCPDS 47-0124) instead of anatase TiO_2, which is confirmed by the peaks at $2\theta = 9.2°$ and 24°. The two peaks correspond well to (2 0 0) and (1 1 0) reflections of $H_2Ti_2O_5{\cdot}H_2O$, respectively. Diffractions that are attributable to anatase phase of TiO_2 crystal (JCPDS 21-1272) are clearly detectable in Sample **b** and **c**. The peaks of titanate do not present in Sample **b** and **c**, and the peak intensity increases. That indicates that the nanotubes' crystal phase changes, and the titanate turns into anatase TiO_2 during the illumination process. It has been reported that the nanotube structure is influence by the crystal phase [12]. So the structure of nanotubes in Sample **b** should have been damaged. Compared with Sample **a**, new peaks at $2\theta = 44°$ and 64° emerge in curves **b** and **c**, which correspond well to (2 0 0) and (2 2 0) diffractions of gold (JCPDS 4-0784), respectively. It proves that gold particles are deposited on the support. No diffraction peaks of $HAuCl_4$ are observed in Sample **b**, which indicates that gold compounds adhered to the TiO_2 support should have decomposed completely after the illumination process. After Sample **b** is calcined, no obvious phase transformation is observed. However, the diffraction intensity of TiO_2 and gold in Sample **c** is higher than that of Sample **b**, which suggests that the calcination process lead to the agglomeration of TiO_2 support and gold particles.

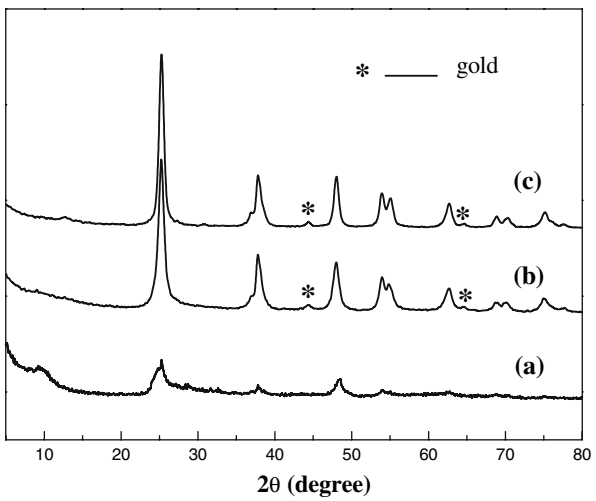

Figure 1. XRD patterns of Samples **a**, **b**, and **c**.

A deep insight into the nanostructure of samples can be obtained by TEM observations. Figure 2 shows the TEM images of Sample **a** and Sample **c**. The typical morphology of the as-prepared titanate nanotubes is displayed in figure 2A and B. Figure 2A indicates that the nanotubes are open-ended, their diameters are nearly uniform and their length is more than 100s of nanometer, similar to the results reported by Kasuga *et al.* [9]. At higher magnification (figure 2B), it can be observed that their diameter is about 10 nm. Wall number of the same nanotube is not identical, which implies that the nanotubes are constructed through scrolling mechanism [13]. Figure 2C and D shows TEM and high-resolution TEM (HRTEM) picture of Sample **c**, respectively. Lamellar particles with size of about 10 nm are well distributed on the linear bundles, and no obvious nanotube is observed in the images. It seems that TiO_2 nanotubes are broken during the illumination process, which similar to the formation process of Pt-loaded TiO_2 nanofibers and Pd-loaded TiO_2 nanofibers [14]. No obvious gold particles are observed in the images. It should be attributed to the high-dispersion of the gold particles. Fringes periodicity of the particles and fibers is 0.353 nm, consistent well with the lattice spacing between {101} planes of anatase TiO_2 crystal. It indicates that the support of Au/TiO_2NFs consists of anatase TiO_2 rather than titanate, which corresponds with the results of XRD. Due to the phase transition of TiO_2 nanotubes, the structure of TiO_2 support is changed from nanotube to fiber and supported particle.

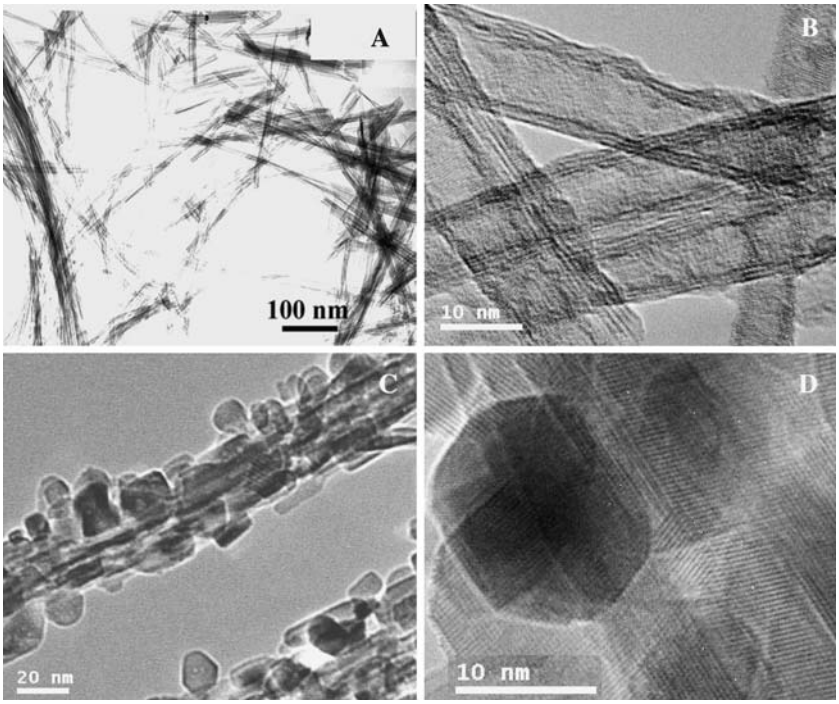

Figure 2. TEM images of Sample **a** (A and B) and Sample **c** (C and D).

So nanofiber instead of nanotube is used as denotation of the catalyst support.

It is commonly accepted that photocurrent can generated and water can be decomposed on TiO_2 electrode [15]. When the TiO_2 is photoexcited by light with energy greater than the band gap of anantase TiO_2, holes and electrons are photogenerated [16]. Photocurrent flowed from the metal counter electrode to the TiO_2 electrode. At the same time, oxidation reaction occurs at the TiO_2 electrode and the reduction reaction at the metal electrode. The scheme is as follows:

$$H^+ + e^- \rightarrow H\bullet \,(\text{at the metal ecletrode})$$

$$2H_2O - 2e^- \rightarrow O_2 + 4H^+ (\text{at the } TiO_2 \text{ electrode})$$

During the photodecomposition process, TiO_2 can be photoexcited due to the high energy of UV light that are generated by High-pressure Mercury Lamp. After gold particles are obtained, small batteries can be formed and H• can be generated. Because of the high surface energy and activity of the nanotubes, some unsaturated O in nanotubes can combine with H• under the excitation of UV irradiation, which may result in the break of Ti–O bonds. As a result, the structure of nanotube is destroyed, and lamellar particles supported on nanofibers form. When the precursor of Au/TiO_2NFs is irradiated, gold particles are formed while TiO_2 nanotubes are broken. The broken support prevents the formed gold particles from agglomerating at the same time. Consequently, small gold particles form, and are difficult to be observed in TEM images.

3.2. Catalytic activity of the prepared catalysts

Au/TiO_2NFs show high catalytic activity for CO oxidation while pure nanotubes exhibit no activity under the same condition. It indicates that gold particles are active centers of the catalyst. Figure 3 shows the catalytic performance of Sample **b** and **c** for CO oxidation. The CO conversion increases with the raise of reaction temperature for the two catalysts. $T_{50\%}$ of Sample **b** and **c** are 123 and 77 °C, respectively. It indicates that Sample **c** has higher catalytic activity than Sample **b**, and the effect of calcination is quite distinct. It has been reported by Haruta that calcinations process is necessary to form strong interaction between gold and the support, and catalytic activity of supported gold is influence by the interaction between gold and the support [17]. Though gold particles are obtained after illumination process, interaction between gold and TiO_2 support is rather weak and the activity of as-prepared Au/TiO_2NFs is relatively low. Stronger interaction between gold and the support can be obtained after calcination process. As a result, heated Au/TiO_2NFs show better catalytic performance.

Figure 4 shows the photocatalytic activities of Sample **a**, **b** and **c**, and catalytic performances of the samples is revealed by the concentration of methyl orange solution and the percent of residual methyl orange at different UV light irradiation time. After irradiation for 3 h, the concentrations of methyl orange solution

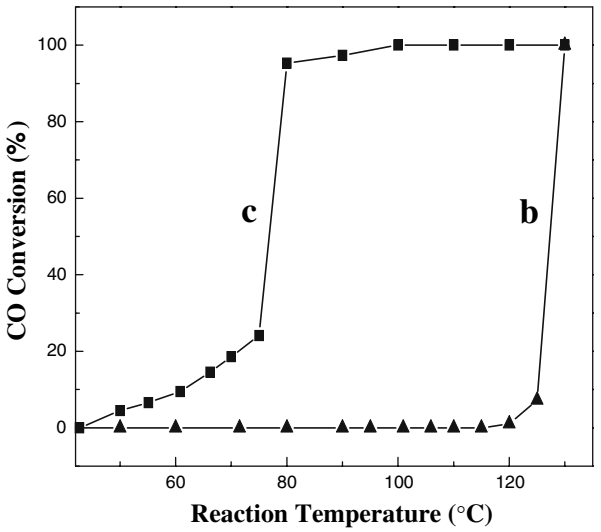

Figure 3. Catalytic activity of Sample **b** and **c** for CO oxidation.

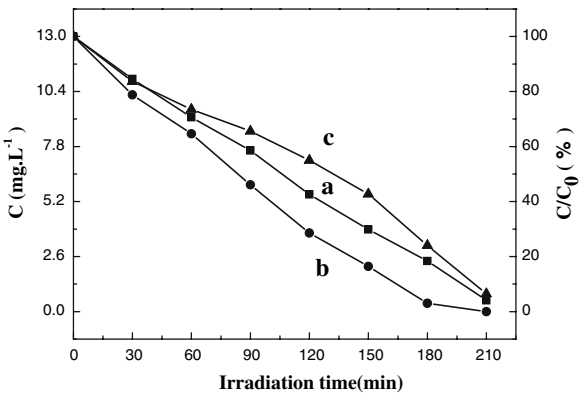

Figure 4. Photocatalytic activities of Samples **a**, **b**, and **c**.

become 4.3, 0.4, 3.1 mg/L in the presence of Sample **a**, **b** and **c**, respectively, which implies that 82%, 97% and 76% of the methyl orange is degraded. It can be seen that pure nanotubes exhibit good photocatalytic performance. After gold is loaded, higher activity can be obtained. In this photocatalytic system, TiO_2 are active centers, and gold particles act as electron acceptor which promotes interfacial charge-transfer processes [18]. However, the photocatalytic activity of Au/TiO_2NFs decreases after the calcination process, which shows distinct difference from the activity for CO oxidation. That should be attributed to the different reaction mechanism of $Au–TiO_2$ system in the two reactions. During the CO oxidation process, gold particles are active centers, and the TiO_2 act as support, which absorb and provide oxygen. After calcination, the stronger interaction between gold particles and support comes into being, which result in high activity for CO oxidation. However, the stronger interaction is in favor of recombination of photogenerated holes and electrons during the photocatalytic process. As discussed above, calcinations also can induce the agglomeration of TiO_2 support and the decrease of photoactive centers. Consequently, the photocatalytic activity of Au/TiO_2NFs decreases after the calcination process.

In conclusion, Au/TiO_2NFs can be prepared by deposition-photodecomposition method and the titanate nanotubes are broken during the fabrication process. The catalytic activity of Au/TiO_2NFs is influenced by the interaction between gold and TiO_2. After Au/TiO_2NFs is calcined, their catalytic activity for CO oxidation is enhanced, while the photocatalytic activities decrease. Different catalytic mechanism of $Au–TiO_2$ system in the two reactions should be the main reason.

Acknowledgments

This work is supported by 973 Program (2005CB623607).

References

[1] M. Haruta, T. Kobayashi, H. Sano and N. Yamada, Chem. Lett. 2 (1987) 405.
[2] T.V. Choudhary and D.W. Goodman, Top. Catal. 21 (2002) 25.
[3] M. Haruta, N. Yamada, T. Kobayashi and S. Iijima, J. Catal. 115 (1989) 301.
[4] M.M. Schubert, S. Hackenberg, A.C.V. Veen, M. Muhler, V. Plzak and R.J. Behm, J. Catal. 197 (2001) 113.
[5] F. Boccuzzi, A. Chiorino and M. Manzoli, Mat. Sci. Eng. C 15 (2001) 215.
[6] I.M. Arabatzis, T. Stergiopoulos, D. Andreeva, S. Kitova, S.G. Neophytides and P. Falaras, J. Catal. 220 (2003) 127.
[7] Y. Tian and T. Tatsuma, J. Am. Chem. Soc. 127 (2005) 7632.
[8] R.S. Sonawane and M.K. Dongare, J. Mol. Catal. A 243 (2006) 68.
[9] T. Kasuga, M. Hiramatsu, A. Hoson, T. Sekino and K. Niihara, Langmuir 14 (1998) 3160.
[10] B.L. Zhu, Q. Guo, X.L. Huang, S.R. Wang, S.M. Zhang, S.H. Wu and W.P. Huang, J. Mol. Catal. A 249 (2006) 211.
[11] B.L. Zhu, X.X. Zhang, S.R. Wang, S.M. Zhang, S.H. Wu and W.P. Huang, Micropor. Mesopor. Mat. 102 (2007) 333.
[12] M. Zhang, Z.S. Jin, J.W. Zhang, X.Y. Guo, J.J. Yang, W. Li, X.D. Wang and Z.J. Zhang, J. Mol. Catal. A 217 (2004) 203.
[13] R. Ma, Y. Bando and T. Sasaki, Chem. Phys. Lett. 380 (2003) 577.
[14] B.L. Zhu, Ph.D. Dissertation of Nankai University, 2006.
[15] A. Fujishima, T.N. Rao and D.A. Tryk, J. Photochem. Photobiol. C 1 (2000) 1.
[16] H. Liu, X.Z. Li, Y.J. Leng and W.Z. Li, J. Phys. Chem. B 107 (2003) 8988.
[17] M. Haruta, S. Tsubota, T. Kobayashi, H. Kageyama, M.J. Genet and B. Delmon, J. Catal. 144 (1993) 175.
[18] V. Subramanian, E. Wolf and P.V. Kamat, J. Phys. Chem. B 105 (2001) 11439.